



Nanostructures in environmental pollution detection, monitoring, and remediation

A. Vaseashta^{a,b,*}, M. Vaclavikova^c, S. Vaseashta^a, G. Gallios^d,
P. Roy^b, O. Pummakarnchana^e

^aNanomaterials Processing and Characterization Laboratories, WV, USA

^bGraduate Program in Physical Sciences, Department of Physics and Physical Sciences, Marshall University, Huntington, WV 25755, USA

^cInstitute of Geotechnics, Slovak Academy of Sciences, 45 Watsonova St., 043 53 Kosice, Slovakia

^dDepartment of Industrial Chemistry and Chemical Technology, School of Chemistry, Aristotle University of Thessaloniki, Thessaloniki, GR-541 24, Greece

^eDepartment of Environmental Science, School of Science, Silpakorn University, Nakornpathom 70000, Thailand

Received 23 July 2006; received in revised form 13 November 2006; accepted 13 November 2006

Available online 2 January 2007

Abstract

We present preliminary results of our joint investigations to monitor and mitigate environmental pollution, a leading contributor to chronic and deadly health disorders and diseases affecting millions of people each year. Using nanotechnology-based gas sensors; pollution is monitored at several ground stations. The sensor unit is portable, provides instantaneous ground pollution concentrations accurately, and can be readily deployed to disseminate real-time pollution data to a web server providing a topological overview of monitored locations. We are also employing remote sensing technologies with high-spatial and spectral resolution to model urban pollution using satellite images and image processing. One of the objectives of this investigation is to develop a unique capability to acquire, display and assimilate these valuable sources of data to accurately assess urban pollution by real-time monitoring using commercial sensors fabricated using nanofabrication technologies and satellite imagery. This integrated tool will be beneficial towards prediction processes to support public awareness and establish policy priorities for air quality in polluted areas. The complex nature of environmental pollution data mining requires computing technologies that integrate multiple sources and repositories of data over multiple networking systems and platforms that must be accurate, secure, and reliable. An evaluation of information security risks and strategies within an environmental information system is presented. In addition to air pollution, we explore the efficacy of nanostructured materials in the detection and remediation of water pollution. We present our results of sorption on advanced nanomaterials-based sorbents that have been found effective in the removal of cadmium and arsenic from water streams.

© 2006 NIMS and Elsevier Ltd. All rights reserved.

Keywords: Nanostructured materials; Pollution; Satellite; Sensors; Water purification; Integrated; Sensor technology

1. Introduction

In a recent study, the World Health Organization (WHO) reported that over 3 million people die each year from the effects of air pollution. Furthermore, reports from World Energy Congress (WEC) suggest that if the world continues to use fuels reserves at the current rate, the

environmental pollution in 2025 will create irreversible environmental damage. Long-term exposure to air pollution provokes inflammation, accelerates atherosclerosis, and alters cardiac function. Within the general population, medical studies suggest that inhaling particulate matter (PM) is associated with increased mortality rates which are further magnified for people suffering from diabetes, chronic pulmonary diseases, and inflammatory diseases. Pollution, in general is contamination that renders part of the environment unfit for intended or desired use. Natural processes release toxic chemicals into the environment as a result of ongoing industrialization and urbanization. Major

*Corresponding author. Nanomaterials Processing and Characterization Laboratories, WV, USA. Tel.: +1 304 696 2755; fax: +1 304 696 2755.

E-mail address: prof.vaseashta@marshall.edu (A. Vaseashta).

contributors to large-scale pollution crisis are deforestation, polluted rivers, and contaminated soils. Other sources of pollution include emissions from iron and steel mills; zinc, lead, and copper smelters; municipal incinerators; oil refineries; cement plants; and nitric and sulphuric acid producing industries. Of the group of pollutants that contaminate urban air, nitrous oxide (NO_x), fine suspended PM, sulphur dioxide (SO_2), and ozone pose the most widespread and acute risks. Recent studies on the effects of chronic exposure to air pollution have singled out PM suspended in smog (NO_x) and volatile organic compounds (VOCs) as the pollutant most responsible for life-shortening respiratory and associated health disorders. Since the Clean Air Act was adopted in 1970, great strides have been made in the U.S. in reducing many harmful pollutants from air, such as SO_2 . Levels of NO_x , however, have increased by 20% over the last 30 years. Sources of NO_x include passenger vehicles, industrial facilities, construction equipment and railroads, but of the 25 million tons of NO_x discharged annually in the U.S., 21% of that amount is generated by power plants alone, resulting in rising threats to the health of the general population. Furthermore, the SCanning Imaging Absorption SpectroMeter for Atmospheric CHartography (SCIAMA-CHY), shows rapid increase in NO_x columns worldwide, especially during 2003–2006.

Sources of contamination in water include processes related to municipal, industry, and agricultural waste, such as water-borne bacteria and Arsenic (As) that enter the watershed. Consequently, rapid detection of contaminants in the environment by emerging technologies is of paramount significance. Environmental pollution in developing countries has reached an alarming level thus necessitating deployment of real-time pollution monitoring sensors, sensor networks, and real-time monitoring devices and stations to gain a thorough understanding of cause and effect. A tool providing interactive qualitative and quantitative information about pollution is essential for policy makers to protect massive populations, especially in developing countries.

On a scientifically related note, inadvertent contamination from extreme natural phenomenon such as hurricanes, epidemics such as avian flu and animal diseases, and deliberate contamination from warfare and terrorism have elevated governmental awareness for methods to detect and sense contaminants in air, water, food, and agricultural supplies. Recent progress in nanostructured materials and their possible applications in chemical and biological sensors will have a significant impact on efficient and accurate data collection, processing, and recognition. In clinical medicine, the current trend is to decentralize laboratory facilities and conduct clinical trials employing direct reading, portable, and lab-on-chip (LOC) systems. Significant research attests to fast, cost-effective, and simple diagnosis of inherited or infectious diseases, and early detection of infectious agents in various environments attributable to the use of nanostructured materials in sensing devices [1].

Although, chemical and biological agents are also classified as contaminants or pollutants, the aim of this investigation is focused towards anthropogenic materials and gases. Large numbers of these materials have dimensions falling within the nanometer range and hence the relevance of nanoparticles and their impact on health, safety and the environment in the context of nanogeoscience is discussed. Nanoparticles broadly fall into two categories: anthropogenic (incidental and engineered) and natural and biological. The topic as to which category of nanoparticles adversely affects the cells and human organisms or even ecosystem, is currently under investigation, under a different context. Several studies conducted by the Earth Policy Institute (EPI), Health Effects Institute (HEI), and the National Institute of Environmental Health Sciences (NIEH) and vast literature from the Journal of American Medical Association (JAMA), American Lung Association (ALS), American Cancer Society (ACS), and similar journals worldwide point out that pollution, irrespective of its origin, can adversely affect the human system and significantly increase deaths from heart disease showing links between air pollution and atherosclerosis. Epidemiologists specifically investigated the effects of PM, a mixture of airborne microscopic solids and liquid droplets that includes acids (such as nitrates), organic chemicals, metals, dust, tail-pipe emission and allergens. Particles less than $2.5\mu\text{m}$ in diameter pose the greatest problems to health as they can penetrate deep into the lungs and sometimes even enter the bloodstream, having immediate and long-term effects on the human organism with varying severities depending upon the individual's existing physical conditions. Global adverse impacts of pollution calls for intense study into its immediate, long and wide range effects thus forming the impetus for our investigation: an environmental information system that detects and monitors air pollution at its source using ground level nanomaterials-based sensors and detects and monitors air pollution dispersion over a wide range using satellite imagery and image processing of satellite data.

A second form of pollution contributing to widespread harm to humans and the ecosystem arises from toxins and similar contaminants found in water. Because of its extreme toxicity, the detection and removal of arsenic in streams and watersheds demands priority in pollution control efforts. Arsenic occurs naturally in rocks and soils, water, air, plants, and animals. Volcanic activity, the erosion of rocks and minerals, and forest fires are natural sources of arsenic release in the environment. As with air pollution, anthropogenic activities are also responsible for arsenic release into the environment. Wood preservatives, paints, drugs, dyes, metals, and semiconductors contain arsenic. Agricultural applications (pesticides, fertilizers), fossil fuel combustion, mining, smelting, land filling, and other industrial activities contribute to arsenic releases as well. These natural and anthropogenic sources introduce a certain amount of arsenic into the environment and increase its concentration and distribution.

It has been reported that As (III) is 4–10 times more soluble in water than As (V) and As (III) is 10 times more toxic than As (V). The presence of arsenic species in drinking water, even in low concentrations, is a severe threat to human health. The WHO recommended the new maximum contaminant level (MCL) of arsenic in drinking water to $10 \mu\text{g L}^{-1}$ from an earlier value of $50 \mu\text{g L}^{-1}$. This greatly reduced limit was recently accepted by authorities of European Union (EU) as well as by United States Environmental Protection Agency (US-EPA) (Directive 98/83/EC 1998; US EPA, 2002). As a part of environmental pollution remediation initiatives, various treatment methods have been developed for the removal of arsenic from water streams. We report a sorption method as a promising, cost-efficient, and stand-alone procedure with the aim of meeting the new target limit. In this work, magnetic nanoparticles have been synthesized and used for sorption studies of arsenic species from model aqueous solutions. A brief mention of air pollution remediation using nanowires masks and nanotube-based static discharge apparatus is also described.

2. Environmental pollution detection and monitoring

Ground-based measurements are usually carried out to monitor urban pollution. Satellite data, however, have traditionally been unexploited by environmental pollution scientists. With the advancement of remote sensing technologies with high-spatial and spectral resolution, it is now possible to model urban pollution using satellite images. Commercially available gas and VOCs sensors provide fairly accurate ground pollution concentrations. Fig. 1 shows a conceptual framework of the proposed integrated tool showing various sources of pollution,

monitoring devices linked to a remote server, and authentication of the ground-based data by satellite data [2].

2.1. Ground-based monitoring

Air pollutant measurements have been carried out with analytical instruments such as optical spectroscopy, gas chromatography, mass spectrometry, non-dispersive infrared (NDIR), and chemiluminescence. Such monitoring systems are bulky, expensive, time-consuming, and can seldom be used for real-time monitoring in the field despite their capabilities of delivering accurate readings. Furthermore, the use of aforementioned systems as stand alone is not practical. Recent development of thin semiconductor films employing nanostructured materials, Nerst-type potentiometric devices based on solid-electrolyte membrane, and NiO/ZnO capacitor-type gas sensors and detectors offer excellent alternatives for environmental monitoring. The devices are low cost, light weight, and relatively small in size. Several different kinds of thin-film sensors are commercially available for detection and monitoring of NO_x gas. For this investigation, low cost, metal-oxide semiconductor junction with Schottky structure-type sensors were used, as one of the goals to install several of these sensors at several locations in the major cities worldwide to monitor ambient NO_x concentration levels in real-time. The WO_3 sensor is a low cost, commercial device that contains a proprietary blend of dopants and catalysts to optimize the sensitivity ($< 0.5\text{--}10 \text{ ppm}$) and selectivity for NO_x gases. The WO_3 sensors were adjusted for zero to maximum scale using a feedback circuit. The sensor was calibrated specifically for NO_x to conduct single gas studies, albeit measurements for

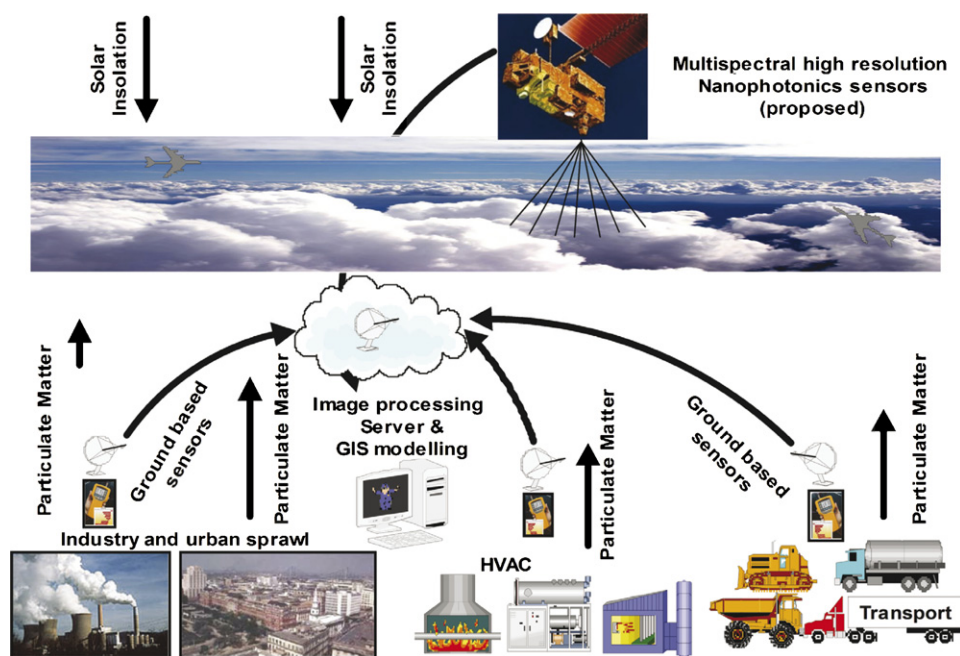


Fig. 1. An integrated atmospheric pollution parameters monitoring unit using ground-based sensors and real-time satellite data and in situ processing.

other pollutants, such as VOC were also conducted. To study the reproducibility response, the response of the sensors with varying concentrations after air purge was conducted, as shown in Fig. 2(a). The WO₃ sensors show an increasing voltage output with increasing NO_x concentrations, as shown in Fig. 2(b). The characteristic of sensor response can be considered as a linear correlation between NO_x gas concentration and V_{out} measured from the sensor. Regression analysis on several data shows an average R² value of ~0.96, indicating a good correlation. The response and recovery time of the sensor is dependent on the NO_x concentrations. The circuitry in the sensor refreshes itself periodically. In addition, different gases were exposed to

the sensors in order to investigate the uniformity of sensor response. The sensor was exposed to NO_x gas in 0–7.54 ppm range to investigate the characteristics of sensor response to varying concentrations. To investigate further the stability characteristics of sensor response to NO_x, the sensor was exposed to pure NO_x gas of 10 ppm for 5 min. The sensors displayed fairly uniform response as seen from the results in Fig. 2(c).

For the present investigation, the NO_x sensors were purchased from the Synkera Technologies Inc., and were inserted in an electronic TO-39 package with analog/digital transducer circuitry to interface the output with a personal digital assistant (PDA) with geographical information

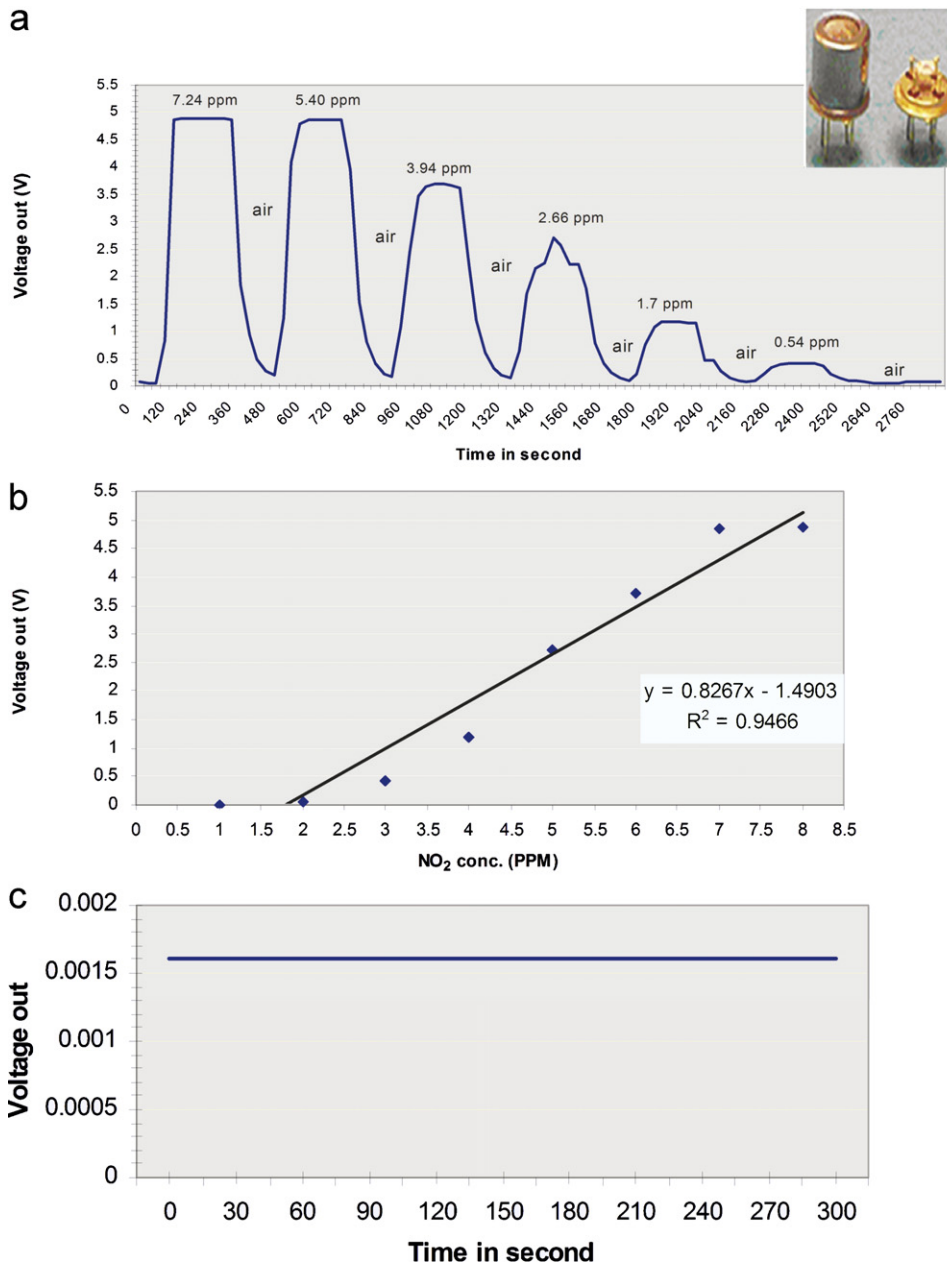


Fig. 2. Sensor response (V_{out}) to varying concentrations of NO_x concentrations, showing: (a) Sensor response to NO₂ in 0.54–7.50 ppm range showing sensitivity and reproducibility. (b) Linear response as a function of gas challenge. (c) Stability of the gas sensor to NO_x (10 ppm). Inset shows a packaged gas sensor.

systems (GIS) capability. The data acquired from monitoring sites are uploaded via a PDA with global positioning system (GPS) capability to a central file-server. The air quality level information is displayed in the form of GIS databases. The topological coordinates of each sensor are superimposed over a map of a location under observation using map server, thus providing a topological layout of pollution of the city in real time. The circuitry for analog to digital (A/D) and digital to analog (D/A), protocol, and logistics for data transfer from sensors to the central file server and map server were optimized for this investigation. To ensure accuracy, the NO_x data are averaged hourly using the Visual Basic programming language, after which SQL facilitates querying of the hourly average of the NO_x data and its subsequent upload to the Postgre SQL database, an open source relational database system hardened to ensure reliability and integrity of the data on the web server. NO_x concentration levels acquired from monitoring sites, GIS maps, satellite image from IKONOS (Greek word for image) and attributes were input into a PDA linked with GPS. The results were utilized for air quality level modeling of the study area. The model developed is used for acquiring and monitoring real-time air quality levels and also for updating information through a wireless GIS using a web map service (WMS) to be displayed in the form of a GIS database. As a pilot project, the air quality levels were overlaid with Bangkok base maps and IKONOS's (4m multispectral, visible bands) image, and the data is displayed on a PDA interface. The three classes of air quality levels reported include low, moderate, and high. Hence, internet users can browse, zoom in, pan, zoom out, and query air quality-based maps, relating to any specific geographic location used as an air quality monitoring (AQM) site. The real-time data is made available to environmental protection personnel to facilitate decision making to ensure appropriate warnings and responses to immediate health threats and more importantly to the general public via web server.

Although commercial gas sensors are used for this investigation, a carbon nanotube (CNT) can be used as a gas sensor, since its electrical characteristics are a strong function of its atomic structure, mechanical deformation, and chemical doping. Any change in the CNT surface can induce a change in conductance, thus making such devices small and sensitive to their chemical and mechanical environment. Sensors made from a single wall (SWNT) have high sensitivity and fast response times even at room temperature. Development of sensors using CNT materials, zinc oxide (ZnO) embedded in polymer matrix [3], and nanoporous materials-based gas sensors is a subject of future investigation. The first principle calculations using density function theory (DFT) on several molecules, such as carbon monoxide (CO), ammonia (NH_3), nitrogen dioxide (NO_2), oxygen (O_2), and water (H_2O), show the direction of the charge transfer and hence the doping of the semiconductor tube [4], which results in change in conductivity. For H_2O , a simulated molecular configura-

tion shows repulsive interaction and no charge transfer in the presence of a water molecule [5], which offers an important option of using SWNTs in water. Furthermore, ionization sensors work by detecting the ionization characteristics of distinct gases; however, they are limited by size and high-voltage operation and large power consumption. The CNTs exhibit excellent field emission characteristics due to the existence of a very large field at the tips even at very low voltages, which could produce compact, battery-powered gas ionization sensors. The field emission-based ionization gas sensors are expected to show good sensitivity and selectivity, unaffected by factors such as temperature, humidity, and gas flow.

2.2. Satellite-based monitoring

The environmental impacts of global warming is an issue that has attracted the attention of scientists, policymakers, and environmentalists. The existence of primary air pollutants viz., SO_2 , NO_x , CO, and methane (CH_4) common in urban and industrialized areas lead to the creation of secondary pollutants by means of photochemical reactions in the atmosphere [6]. In addition, nitric acid (HNO_3) plays an important role in earth's atmosphere as a reservoir molecule of NO_x species in the stratosphere. NO_x species react with each other and with atmospheric water vapor thus forming an extensive system with abundant chemical interplay. Several chemical equilibriums take place, resulting into the formation of new, although connected species, such as nitrous acid (HNO_2) and HNO_3 . It turns out that the role of HNO_3 is central in various master physio-chemical processes occurring in our atmosphere [7].

Aerosol haze scatters, absorbs, and backscatters solar radiation and emits and/or absorbs long-wave (infrared) radiation thereby changing the radiation fluxes at the surface and the top of the atmosphere that significantly perturbs the atmospheric absorption of solar radiation [8]. The appearance of a pollution layer with more absorption and scattering causes a decrease of the atmospheric transmission factor that causes a decrease of solar radiation impinging on the ground. Hence emitted radiance is lower and the signal sensed by satellite is lower. A pollution layer in atmosphere absorbs as well as emits radiance, causing a depletion of the upward radiance. Aerosol climate forcing is the hardest problem for climate modelers because its forcing details are very uncertain [9]. Studies have found that biomass burning contributes significantly to aerosol concentration. Observatory and satellite data revealed that black carbon and fly ash contribute more to haze in Asia than SO_2 [9]. The biomass burning aerosols having dimension of a $0.1\ \mu\text{m}$ are activated in the cloud, consequently cloud condensation nuclei (CCN) properties of these aerosols control their influence on cloud albedo. Scattering albedo increases, as pollution increases, and also backscatter fraction decreases as pollution increases. There is observational evidence that

these aerosols can alter cloud properties. Aerosol radiative forcing depends on hygroscopicity, which in turn depends on aerosol chemistry. Condensation of secondary organic aerosol on nucleation reduces the hygroscopic properties of particles resulting in a slow conversion of cloud drops into precipitation thus allowing the convective energy to accumulate and eventually trigger violent storms. Similarly, by reducing aerosol pollution, or reducing the effect of small pollution aerosols by introducing large hygroscopic elemental aerosols, the early onset of rain is accelerated [10].

Ground-based measurements are usually deployed to monitor urban pollution. The U.S. EPA, some state agencies such as the Texas Commission on Environmental Quality (TCEQ), and many international entities such as France's AIRPARIF, the Netherland's National Institute for Public Health and Environment (RIVM), and government agencies in China and Thailand forecast air quality via website. Several agencies in the EU such as the Natural Environmental Research Council's (NERC) Designated Data Center of the British Atmospheric Data Center (BADC) and Centers for Atmospheric Science (NCAS) assist researchers in locating, accessing, and interpreting current and historical atmospheric data. Using the differential optical absorption spectroscopy-method (DOAS) algorithm, University of Bremen scientists have analyzed the data of the global ozone monitoring experiment (GOME) on ERS-2 and the SCIAMACHY on ENVISAT to retrieve NO_2 columns from SCIAMACHY spectra with high accuracy in the 425–450 nm regions. The objective of our investigation is to extract air pollutants from satellite images using high-spatial and spectral resolution images from advanced spaceborne thermal emission and reflection radiometer (ASTER) in order to assess the level of air pollution by using thermal infrared bands (TIR) and short wave IR (SWIR) bands. As part of our ongoing investigation, we have compared the satellite data with the EPA air quality and spectroscopic study data of atmospheric pollution.

The task of any remote sensing system is to detect radiation signals, determine their spectral character, derive appropriate signatures, and inter-relate the spatial positions of the classes they represent. The remote sensing of atmospheric pollution over land, however, is a challenging task. Multispectral satellite data over land have different responses at different wavelengths, as gases absorb electromagnetic energy in very specific regions of the spectrum. ASTER is an imaging instrument flying on the Terra satellite as part of NASA's earth observing system (EOS). It is the only high-spatial resolution instrument on the satellite that has 14 bands from the visible to the thermal infrared region. In the visible green and near-infrared (V-NIR) between 0.52 and 0.86 μm , there are three bands with 15 m resolution. In the SWIR between 1.6 and 2.43 μm , there are six bands with 30 m resolution. In the ThIR between 8.125 and 11.65 μm , there are five bands with a resolution of 90 m.

ASTER acquires data over a 60 km swath of which the center is pointable.

The data as observed from satellite is processed employing the multivariate techniques, which are based on groupings in a multivariate data set. ER MapperTM has the ability to accomplish this through a series of cluster algorithms. To distinguish between pollution concentration and atmospheric scattering by large-sized dust particles created by urban sprawl, change detection analysis (CDA) on temporal data from LandsatTM 1–7 is used in the investigation. GIS Software ArcGIS (v.9.x) and ArcInfo Workstation from the Environmental System Research Institute (ESRI) are employed to process the satellite data into useable formats. Remote sensing software ER-MapperTM (v.7.x) is further employed to accurately model the data through feature extraction processes for pattern recognition. Several digital imaging processes such as geometric image registration, radiometric normalization, principal component analysis (PCA), and data fusion are employed to process the image for accurate feature extraction. Multivariate correlations and regression analysis methods are used for individual gases with satellite-recorded reflectance of bands.

Fig. 3(A–D) shows the satellite images for four cities (Los Angeles, U.S.A., San Francisco, U.S.A.; Kolkata, India, and Bangkok, Thailand) at 60 km swath [2]. The images illustrate haze layers or smog related to anthropogenic activities. Reflectance, scattering, and absorption of particulates and aerosols can range in size from approximately 0.2 μm onwards, based on the wavelength ranges of the satellite sensors. To accentuate various spectral features, several image processing techniques were used. Data fusion is a method that employs a combination of multi-source data with different characteristics such as spatial, spectral, and radiometric to acquire high-quality image. The integration of spectrally and spatially complementary remote multi-sensor data facilitates visual and automatic image interpretation. To effectively utilize the ASTER images having high-spectral resolution and moderate spatial resolution, data fusion techniques are applied using ER-Mapper 7.x software, so that it can effectively combine into one color image and to preserve spectral characteristics while increasing spatial resolution to provide images of greater quality. The resultant image is further processed into two separate methods: (a) PCA and density slicing (DS). PCA is a decorrelation procedure which reorganizes by statistical means the digital numbers values from as many spectral bands as we choose to include in the analysis. DS is a form of selective one-dimensional classification. The PCA technique involves a mathematical procedure that transforms a number of (possibly) correlated variables into a (smaller) number of uncorrelated variables called principal components. With DS, the continuous pseudo-color scale of the resultant image is "sliced" into a series of classifications based on ranges of brightness values. All pixels within a "slice" are considered to be the same information class. This method is especially

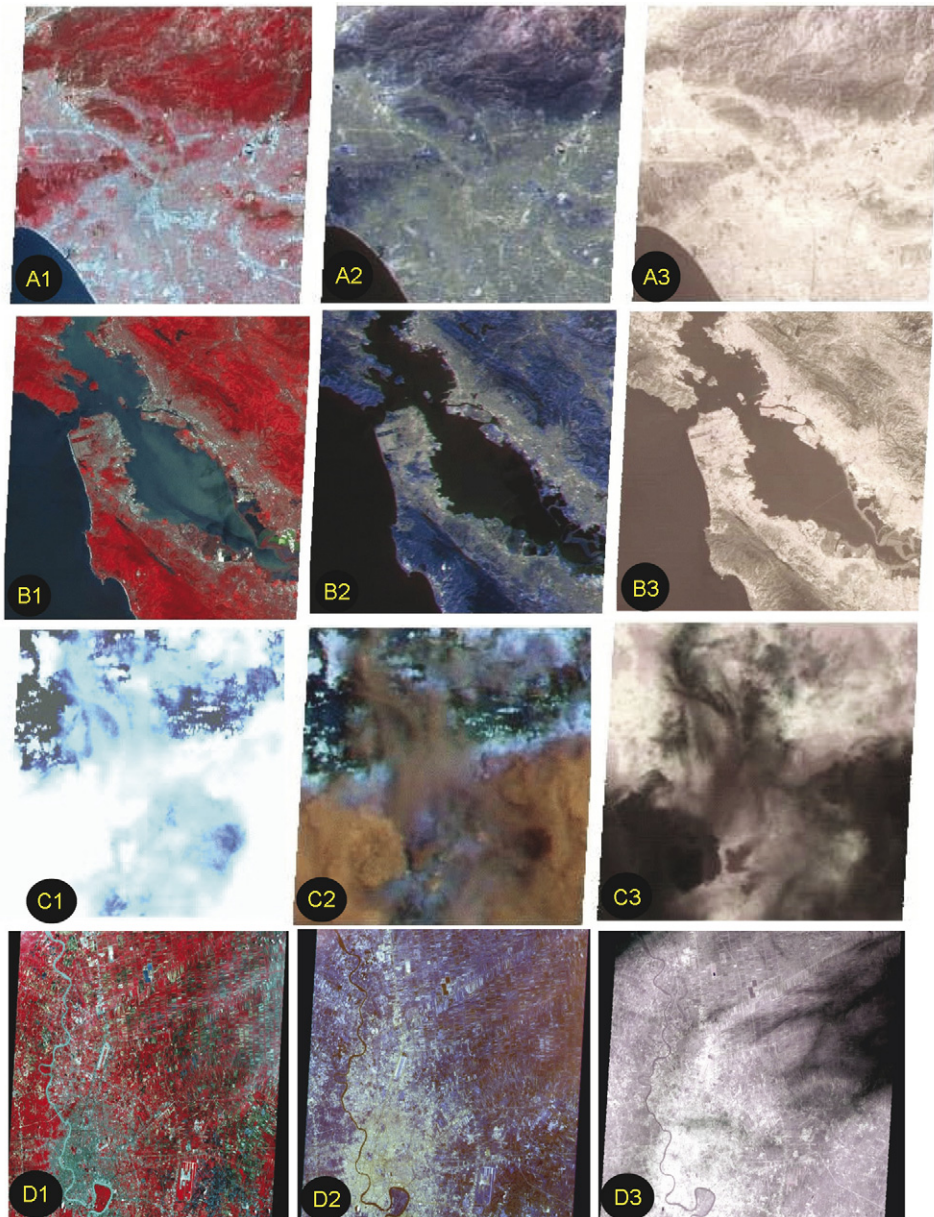


Fig. 3. ASTER data of satellite image of four cities at 60 km swath (Los Angeles, US; San Francisco, US; Calcutta, India; and Bangkok, Thailand), shown in V-NIR, SWIR and ThermalIR.

useful when a given surface feature has a unique and generally narrow set of DN values. Several satellite images were analyzed for this investigation.

As an illustration of image processing, Fig. 4 shows the four cities mentioned above with different image processing methodologies. Fig. 4(1a) shows Los Angeles (LA) industrial area ASTER raw image in RGB bands 321. Fig. 4(1b) shows the same site image processed using PCA in bands 1–14 RGB PC3_PC2_PC1 showing absorption of radiation in the atmosphere due to pollutants. Fig. 4(1c) shows the site using DS in band 14 in pseudo-color over digital orthophoto quarter-quadrangle (DOQQ) confirming the PMs concentration in the atmosphere. Fig. 4(2a) shows San Francisco Bay area image in RGB bands 321. Fig. 4(2b) shows image processing using PCA in bands

1–14 RGB showing smog over Berkeley industries. Fig. 4(2c) shows image processed using DS band 14 over DOQQ confirming the existence of PMs in the atmosphere. Fig. 4(3a) shows ASTER Kolkata, India image in RGB 321 bands. Fig. 4(3b) shows image processing using PCA in RGB showing haze over the city. Fig. 4(3c) is image processed using band ratio in RGB B-3–2, 9–6, 10–14, confirming the presence of PM over the city. Fig. 4(4a) shows Bangkok ASTER image in RGB 321 indicating haze over the NW part of the city. Fig. 4(4b) shows ASTER image in RGB 765 displaying absorption of radiation in SWIR bands and Fig. 4(4c) shows ASTER image in RGB 15, 14, 13 indicating absorption in TIR bands which confirms PM in the atmosphere. Further image processing of two other cities under investigation is shown in Fig. 5,

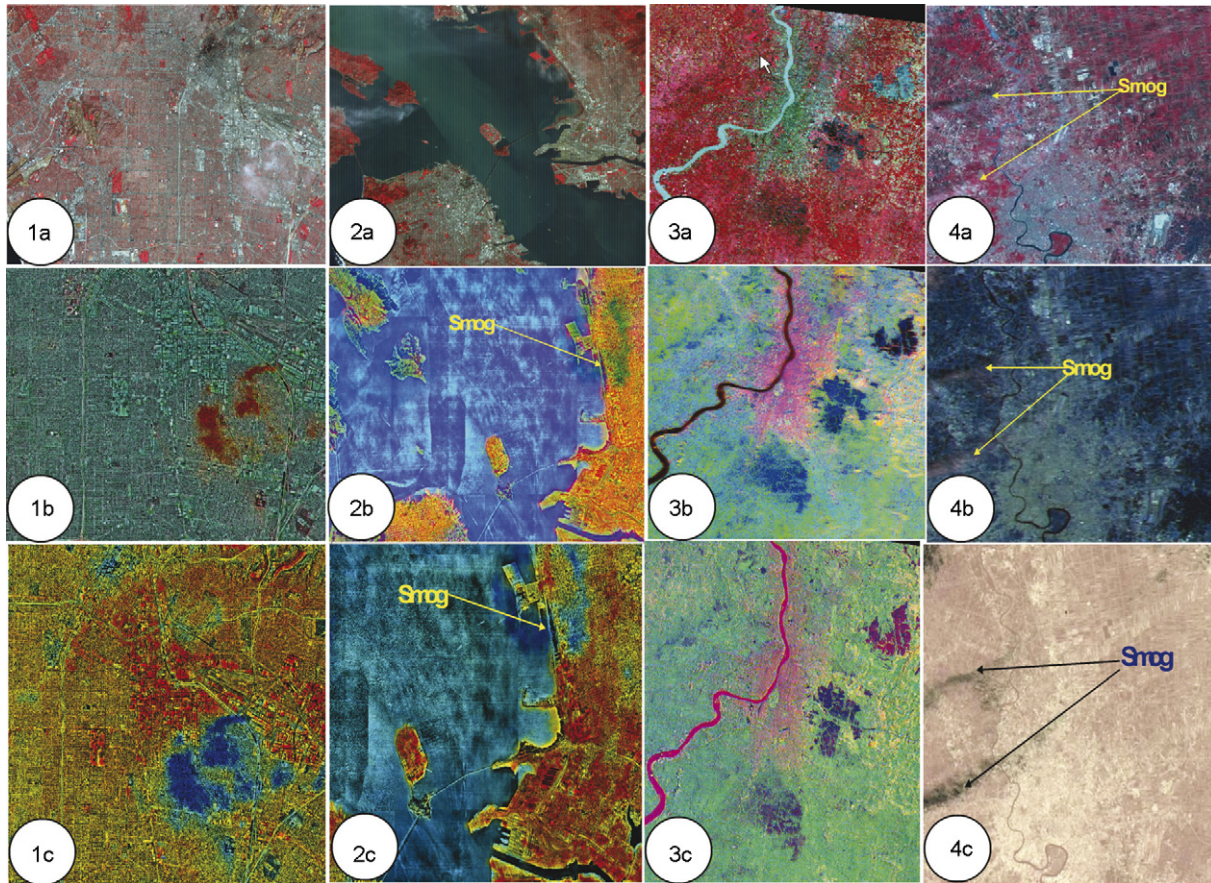


Fig. 4. ASTER satellite images: (1a) LA industrial area ASTER raw image in RGB bands 321. (1b) LA industrial site ASTER PCA B-1–14 RGB PC3_PC2_PC1 shows absorption of radiation in the atmosphere due to pollutants. (1c) LA density slicing band 14 (at $11\ \mu\text{m}$ spectral band) in pseudo-color over DOQQ confirms the particulate matters concentration in the atmosphere. (2a) ASTER San Francisco Bay area image in RGB bands 321. (2b) ASTER PCA 1–14 RGB PC3, PC2, PC1 image shows smog over Berkeley industries. (2c) Density slicing band 14 over DOQQ confirms the existence of particulate matters in the atmosphere. (3a) ASTER Kolkata (India) image in RGB 321 bands. (3b) PCA image Kolkata in RGB PC3, PC2, PC1 shows little haze over the city. (3c) Band ratio image of Kolkata, in RGB B-3–2, 9–6, 10–14, confirms the presence of particulate matters over the city area in either sides of the river Hooghly. (4a) Bangkok ASTER image, in RGB 321 shows haze over the NW part of the city. (4b) Bangkok ASTER image in RGB 765 shows absorption of radiation in SWIR bands. (4c) Bangkok ASTER image in RGB 15,14,13 shows absorption in TIR bands confirm particulate matters in the atmosphere.

which shows ASTER satellite images from (i): Houston showing in Fig. 5(a) PCA in RGB PC 321 of oil refineries; Fig. 5(b) shows band ratio image in RGB 3–2, 9–6, 10–14 showing VOCs; and Fig. 5(c) shows SWIR bands 10,6,5,4 compared. Similarly for Charleston, WV, U.S.A., Fig. 5(d) shows PCA RGB PC 321 showing pollutants; Fig. 5(e) shows image processing using band ratio in RGB 3–2, 9–5, 10–14 clearly showing PM; and Fig. 5(f) the TIR bands 14 and 10 compared thus confirming absorption at $11\ \mu\text{m}$ due to PM, as marked in the images. Similar investigations for several other cities are in progress and will be published in an article exclusively devoted to satellite image processing.

2.3. Environmental information system security issues

Within our investigation, satellite images are acquired from the ASTER imaging instrument on NASA's EOS Terra Satellite from an outside source that are then transmitted to an internal server for image processing and overlay with in situ data. Satellite communications

occur between mobile users, gateways, a Network Control Center, and other satellites. As an information asset supporting research and AQM and remediation directives, it is imperative that satellite image data maintain the highest level of integrity and availability. Within any information system, channels of communication, transmission, processing, and storage introduce vulnerabilities for threats against confidentiality, integrity, and availability of information assets. To circumvent threats from unauthorized access and manipulation of satellite image data, third party geospatial data providers must use authentication within their system. Methods for assuring mutual authentication and data confidentiality between mobile users and satellites include the use of public-key cryptosystems using symmetric (secret) keys, mobile user registration and authentication systems providing secret keys for encrypting transmissions across secure channels, a three-phase authentication protocol including a registration phase, mobile authentication phase, and mobile update phase, and an authorization model for geospatial data that allows

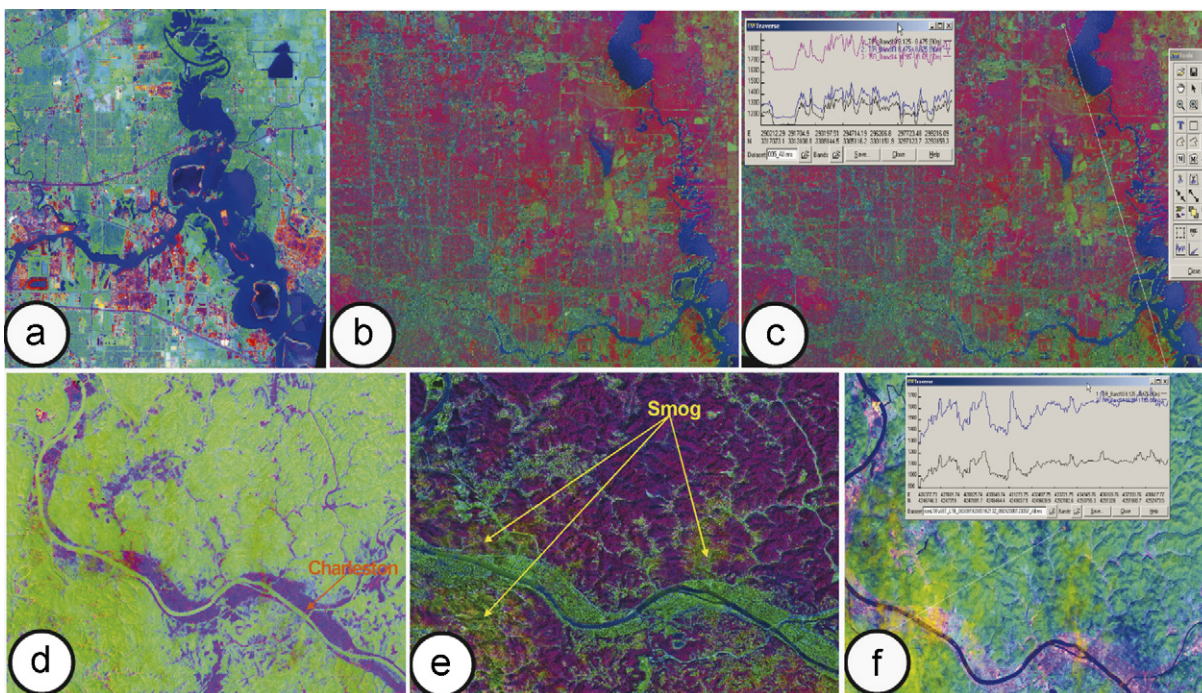


Fig. 5. ASTER satellite images from (i) Houston: (a) PCA in RGB PC 321 of oil refineries. (b) Band ratio image RGB 3–2, 9–6, 10–14 showing VOCs. (c) SWIR bands 10,6,5,4 compared: (ii) Charleston: (d) PCA RGB PC 321 showing pollutants. (e) Band ratio RGB 3–2, 9–5, 10–14 clearly showing PM. (f) TIR bands 14 and 10 compared confirm absorption at 11 μm .

complex authorization policies based on who is accessing the geospatial data at what resolution from what geographic location [11–14].

Within our investigation, environmental data from in situ and satellite sources is processed and stored on database servers accessed within a local area network. To advance the security goals of controlled access, integrity, confidentiality, and availability; we have conducted qualitative and quantitative security risk analyses using Peltier's FRAAP information security risk analysis [15] and Sahinoglu's security-meter [16] information risk analysis, respectively. Our risk analyses helped to identify existing threats and countermeasures improving our security posture that included hardening server services and access, development of an information security policy, and investment in a Symantec Gateway Security 360 firewall. Our information security policy now requires more stringent controls on database access and authentication methods, and practices to ensure that the database is semantically correct, with regular backup and recovery techniques. Finally, future information security plans will invoke technologies that store and verify user credentials and certificates digitally and create user profiles to define access and authorization.

3. Environmental pollution remediation

3.1. Water and soil contamination remediation

Pure water is a very limited natural resource falling short of increasing demands for appropriate quality for indus-

trial and home use. Many pollutants in water streams have been identified as toxic and harmful to the environment and human health. Because of its extreme toxicity, the detection and removal of Arsenic from streams and watersheds demands priority in pollution control efforts. Arsenic is found in the natural environment in some abundance in the Earth's crust and in small quantities in rock, soil, water and air, and to some extent in living animals, plants and microbes. The quantities depend on the level of local contamination and on the type of organism, as certain organisms tend to accumulate arsenic in their bodies. Arsenic is generally present in sea-living animals at higher levels than in freshwater animals, or plants and animals that live on land. It is present in many different minerals and about one third of the arsenic in the atmosphere comes from natural sources, such as volcanoes, forest fires, and the rest comes from man-made sources. Due to natural geological contamination, high levels of arsenic can be found in drinking water that has come from deep drilled wells. Anthropogenic activities are also responsible for arsenic release. Wood preservatives, paints, drugs, dyes, metals, and semiconductors contain arsenic. Agricultural applications (pesticides, fertilizers), fossil fuel combustion, mining, smelting, land filling, and other industrial activities contribute to arsenic releases as well. These natural and anthropogenic sources introduce a certain amount of arsenic to the environment and increase its concentration and distribution. Arsenic is found at higher levels in underground sources of drinking water than in surface waters, such as lakes, reservoirs, and rivers. Water containing 300–4000 $\mu\text{g L}^{-1}$ of arsenic is not so rare

[17,18], as has been observed in water streams closer to industrial zones in some developing countries. Several studies have linked long-term exposure to small concentrations of arsenic with cancer and cardiovascular, pulmonary, immunological, neurological, and endocrine effects. Consequently, there is a tremendous demand for developing efficient methods for removing highly toxic arsenic from drinking waters [19]. It has been reported that As (III) is 4–10 times more soluble in water than As (V) (US EPA-542-S-02-002, 2002) [20]. Moreover, it has been found that As (III) is 10 times more toxic than As (V). Since the presence of even low concentrations of arsenic species in drinking water is a threat to human health; the WHO recommended the new MCL of arsenic in drinking water to $10 \mu\text{g L}^{-1}$ from an earlier value $50 \mu\text{g L}^{-1}$ (WHO, 2004) [21]. This greatly reduced limit was recently accepted by authorities of EU as well as by the US-EPA (Directive 98/83/EC 1998; US EPA 2002) [20].

Various treatment methods have been developed for the removal of arsenic from water. These techniques include nanofiltration (NF) and sorption/ion-exchange [22–24], precipitation [25], coagulation and flocculation [26–29], reverse osmosis (RO) [30,31], membrane technologies [19,26,32], electro-dialysis (ED) [33], biological processes [34] as well as lime softening [35]. While the aforementioned techniques are effective in removing arsenic species from aqueous media, they are costly and very often ineffective in reaching the regulatory limit of $10 \mu\text{g L}^{-1}$. Sorption methods are still considered promising, especially when a cost-efficient procedure is sought and new sorbents are being developed with the aim of obtaining the new target limit.

Sorption on iron (III) oxides, such as amorphous hydrous ferric oxide (FeOOH), poorly crystalline hydrous ferric oxide (ferrihydrite) and goethite (α -FeOOH) have been found to be effective in removing both As (V) and As (III) from aqueous solutions [36–39]. These sorbents can also be easily synthesized from cheap raw materials and possess fairly uniform chemical and physical properties

[40]. As sorption in columns is an established process, the preparation of an effective and relatively cheap sorbent based on iron oxides would make sorption attractive for use in small community systems. Preliminary results with synthetic akaganeite (β -FeOOH) have shown that the maximum capacity of the sorbent is around 75 mg of As per gm of akaganeite, while the results reported in the literature so far have an average value of less than 20 mg As/g of sorbent. This shows that akaganeite is an effective material for the removal of arsenic from water streams. Also, quite good results were obtained with synthetic magnetite/maghemite, with a maximum capacity of ca. 40 mg of As per gm of sorbent. The main problem at the moment is that these are nanomaterials with small particle size (around 20–50 nm) and are not suitable for sorption columns. However, with magnetite/maghemite, which is a magnetic material solid/liquid, separation can be easily done in a high gradient magnetic field. One of the methods under investigation is to incorporate selected nanomaterials into a well-organized host. Nanoporous and microporous crystals, such as molecular sieves (zeolites) are ideal hosts for accommodation of organic and inorganic molecules, polymer chains, and so on due to their uniform pore size and their ability to absorb molecular species, as shown in Fig. 6(a). The incorporation of iron oxides/oxyhydroxides-based nanostructures to zeolites would produce a novel sorbent, which will have both required capabilities: high capacity for arsenic removal and suitable size for use in sorption columns. Our preliminary results with magnetically modified natural zeolite have shown that our new composite material has significant sorption capacity of arsenic ca. 50 mg of As per gm of sorbent. In this work, magnetic nanoparticles have been synthesized and used for sorption studies of arsenic species from model aqueous solutions. Batch-type experiments have been performed in solutions with initial concentrations of arsenic in the range of 20–200 mg L^{-1} and sorbent dosage of 2 g L^{-1} . All sorption experiments were carried out at ambient temperature ($22 \pm 1^\circ\text{C}$) in an orbital shaker at pH

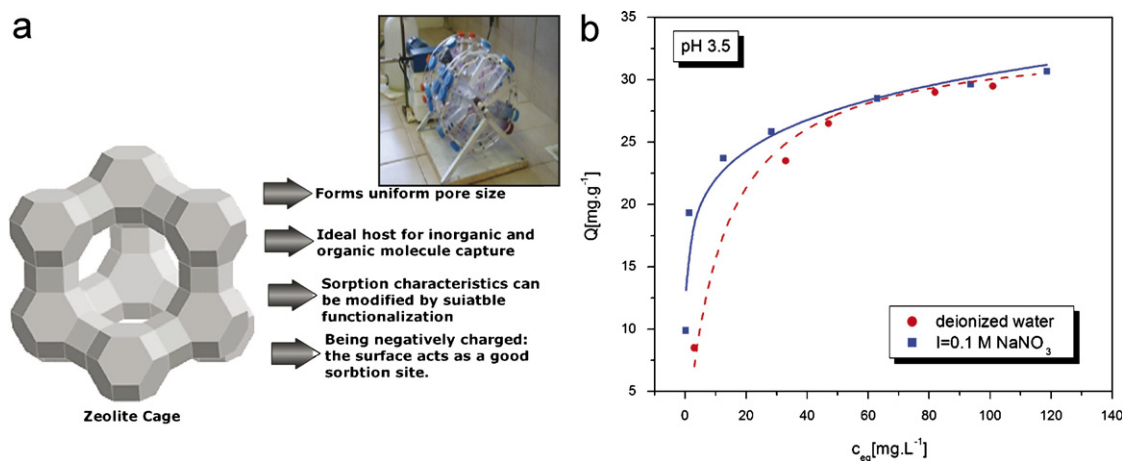


Fig. 6. (a) Zeolite as an ideal hosts for accommodation of organic and inorganic molecules, polymer chains, etc. (b) Arsenic uptake by magnetite nanoparticles. Inset shows a prototype filtration device.

Table 1
Sorption parameters used in modeling

| <i>Langmuir parameters</i> | | | |
|------------------------------|----------------------------------|------|-------|
| De-ionized water | Q_{\max} (mg g ⁻¹) | K | R^2 |
| | 33.44 | 0.09 | 0.97 |
| <i>Freundlich parameters</i> | | | |
| 0.1 M NaNO ₃ | K | b | R^2 |
| | 15.91 | 0.14 | 0.94 |

3.5. The effect of ionic strength on As removal was examined using 0.1 M NaNO₃ as electrolyte. Experimental data were modeled with Langmuir and Freundlich-type sorption isotherms. The corresponding data and model isotherms are shown in Fig. 6(b).

The maximum removal capacity is over 30 mg of As/g of magnetite, which is an above average value presented in the literature. As the initial As concentration increases, there is a steep increase in the amount of As removed per gram of solid (Fig. 6(b): initial curve up to $c_{\text{eq}} = 30 \text{ mg L}^{-1}$). With further increase of the initial As concentration, the slope of curves decreases until it becomes almost constant at the point where equilibrium is almost reached. The type of the curves is similar to Freundlich and Langmuir sorption models and the results were modeled accordingly. The data of the modeling operation are presented in Table 1. The data without electrolyte were fitted better with Langmuir model. The coefficient of determination R^2 was 0.97 showing a good agreement of the model with the experimental data. In the case of experiments with 0.1 M NaNO₃ electrolyte, the data were satisfactorily fitted by a Freundlich equation ($R^2 = 0.94$). Moreover, no significant effect of ionic strength is obvious from results given in Fig. 6(b). Inset in Fig. 6 shows a prototype orbital shaker filtration device in our laboratories in Slovakia. Taking into account the magnetic nature of magnetite and the very easy S/L magnetic separation, these results are very promising. Since magnetite nanocrystals (NCs) respond to low magnetic fields in a size-dependent manner, separations at very low magnetic fields (<100 T/m) is applied to purification columns to increase overall efficiency of the removal of toxic metal contaminants. Similar techniques, along with nanofiltration, nanocatalysis, and nanosorbents are currently used to ameliorate other toxic metal ions, radionuclides, organic and inorganic solvents, bacteria and viruses.

3.2. Air pollution remediation

The necessity for abundant clean water supplies is complemented by a need for clean air in order to improve the quality of life for millions of people worldwide. Gases such as NO, NO₂, CO₂, SO₂, CH₄, CO, and aerosols, and automobile emissions are atmospheric particulates for which the generation, transport, and interaction and chemical affects on the human body are not well understood. As mentioned above, several organizations recog-

nize that particulates and nanoparticles, irrespective of source, play a role in degrading human respiratory systems. The need to understand the transport of nanoparticles is particularly important in view of the threat we face due to inadvertent or intentional introduction of chemical warfare agents (CWA), radioactive fallout from a “dirty bomb”, and biological agents (e.g. anthrax spores). Understanding the transport rates may provide a critical vector for possible distribution of these chemical, biological, and radiological agents and may even apply to VOCs, air borne bacteria, and viruses.

Given the above scenario, we have focused our research on air pollution remediation systems for purifying an individual’s surrounding environment with personal health care devices. In one case, we have employed the CNT filled in a polymer composite matrix [3] to create a static discharge to remove the PM from incoming air. Several products using static discharge are currently being commercialized; however, the CNT-polymer mix electrode provides ionization at a reduced voltage and stronger adhesion of the PM to the electrodes. We have further employed electrospun fibers for system on fibers (SOF) [3], in chemical protective clothing and breathing filtration masks. The process of electrospinning for fiber preparation provides a unique possibility to produce fibers of varying porosity and thus a high surface area. The high surface area/volume ratio combined with its potential biocompatibility and biodegradable nature offers tremendous promise for diverse biomedical applications.

We have attempted several synthetic and natural polymers, polymers composites, polymers impregnated with nanoparticles, CNTs, and compounds for mechanical, electrical, and biological applications using single and multiple jet electrospinning apparatus. A typical electrospinning apparatus consists of a microprocessor-controlled syringe pump with high metering precision at a low, pulse-free pre-set rate and volume control. The internal diameter of the syringe is used by the control program to calibrate the pump and deliver a pre-determined volume and flow rate. The electric field is applied with a high-voltage (30 kV) power supply by connecting the metal discharge needle and a ground stationary or rotating electrode. The strong electric field on a polymer fluid generates an electrostatic force on the surface against the viscous stresses of the polymeric mass, thus producing jets towards the other electrode. A Taylor cone [41] is generated in the jet when a hydraulic effect produced by the syringe plunger to the polymer solution is modified by the strong electrostatic field. The shape of the cone, employing parameters such as viscosity; conservation of mass, charge, and momentum; electric field; surface tension; air drag; and Coulombic and gravitational forces has been modeled by several investigators. For filtration applications, the highly porous structure of the fibers combined with a large surface area renders them ideally suited for aerosol filters, facemasks, and protective clothing. The ability to develop polymer composites, ceramers, electro-ceramers, and bio-ceramers

with varying characteristics such as a large surface area, porosity, bio-compatibility, mechanical strength, and so forth offers tremendous potential to develop fibers with desired shapes and characteristics, resulting in many hybrid components. For the present investigation, the fibers under study consist of multilayer arrangements of patterned fibers deposited on air-permeable substrates. Experiments are in progress to test the filtration efficiency, air flow characteristics, and the effects of loading on filtration and air flow characteristics of these fiber deposited substrates with an ultimate goal for inclusion in garments for specific occupations such as coal-mining, soldiers' suits for complete protection from chemical and biological agents, and workers in highly polluted industrial environments.

4. Conclusions and future directions

Preliminary investigations to correlate pollution data observed from ground-based sensors and image-processed satellite images is presented. The sites under current observation are Los Angeles, CA, U.S.A.; San Francisco, CA, U.S.A., Kolkata, India, and Bangkok, Thailand. VOC emission and smog were also observed from Houston, TX, U.S.A. and Charleston, WV, U.S.A.—both known for oil and chemical refineries; using satellite images and correlated with data obtained with local emission monitoring agencies. Ground as well as satellite data indicates increased smog and VOC levels for the cities under observation. An extension of this project will include several major cities around the world. To reduce the harmful effect of environmental pollution in air and aquatic systems, air filters using activated polymer fibers are prepared. Air filtration efficiency of such filters is under investigation. For aquatic systems, iron oxides/oxyhydroxides-based nanostructures embedded in zeolites were studied. Such structures have high capacity for arsenic removal and are suitable in size for use in sorption columns. Preliminary results with magnetically modified natural zeolite have shown that our new composite material has significant sorption capacity of arsenic ca. 50 mg of As per gm of sorbent. Experimental data were modeled with Langmuir and Freundlich-type sorption isotherms.

Future success in pollution remediation throughout the world demands the development of novel and complex sets of materials and devices. Nanoscience and nanotechnology addresses some of the greatest challenges of the 21st century by providing routes to synthesize materials by design and establishing connection between structure and function of biomolecules to human physiology. Many technologists have developed new tools, yet they often have limited understanding of the needs of biomedical communities or the restrictions that biology places on the proper design of nanotools and nanosystems. More specifically, the physico-chemical kinetics in nanostructured systems explains the interaction of gases, liquids and biological media, leading to its application for a wide variety of

environmental and biomedical functions. Hence, these new materials promise a cornucopia of new products with superior performance characteristics that will dramatically transform markets in a number of key industries. However, further advances are necessary to entirely understand, characterize, develop, and optimize the properties of these recent nanoscale materials, devices, and systems. Since nanomaterials are ideal building blocks for the fabrication of structures, nano-devices, and functionalized surfaces; one of the key challenges for such applications is to precisely control the growth of these materials at desired sites with a desired structure and orientation. Despite the aforementioned challenges, the present investigation presents a convincing argument for an imminent and ongoing need to develop nanoscale materials, devices, and systems for sensing, monitoring, and remediating environmental pollution. Specific to remote sensing via satellite, advances in nanophotonics will enhance the resolution limits of satellites, thus providing details and enhanced feature extraction capabilities. Future pollution remediation nanomaterials-based techniques may include pollution transport by nanoparticles which will have medical, radiological, and even national defense implications in terms of human health, safety, and the environment. Ontological approaches towards studying and understanding the interaction of nanoparticles with the human body, nanoparticles dynamics in air and aquatic systems, composition-dependent disposition and dispersion of nanoparticles, short- and long-term effects of nanomaterials with the human body, immunotoxicity and phototoxicity of nanoscale materials will address some of the societal issues of nanotechnology.

Acknowledgments

The authors would like to acknowledge suggestions on image processing from Mr. J. Barrios and Prof. J. Brumfield of the Geobiophysical Modeling Group at Marshall University, WV, USA. The financial support of NATO (Collaborative Linkage Grant EST.EAP.CLG 981103) and Slovak Science and Technology Assistance Agency (contract No. APVT-51-017104) is greatly acknowledged.

References

- [1] A. Vaseashta, D. Dimova-Malinovska, J.M. Marshall, *Nanostructured and Advanced Materials*, Springer, Dordrecht, The Netherlands, 2005.
- [2] A. Vaseashta, in: *Proceedings of the First International Workshop on Semiconductor Nanocrystals, SEMINANO 2005*, Budapest, Hungary, 2005, 139pp.
- [3] A. Vaseashta, A. Erdem, I. Stamatina, in: *Proceeding of the MRS*, Spring 2006, San Francisco, CA, 2006.
- [4] J. Zhao, A. Buldum, J. Han, J.P. Lu, *Nanotechnology* 13 (2002) 195.
- [5] P.G. Collins, K. Bradley, M. Isigami, A. Zettl, *Science* 287 (2000) 1801.
- [6] UNEP Assessment Report, vol. I, URL: <http://www.rrcap.unep.org/abc/impactstudy/Part%20I.pdf>.

- [7] M. Winnewisser, A. Perrin, J. Orphal, *J. Mol. Spectrosc.* 228 (2004) 375.
- [8] V. Ramanathan, M.V. Ramanna, Atmospheric brown clouds; long-range transport and climate impacts, *EM* December, 2003.
- [9] Y.S. Lee, D.R. Collins, R.A. Farrare, in: Proceedings of the 23rd Annual American Association for Aerosol Research Meeting, Atlanta, GA, October 2004.
- [10] T. Petaja, V.M. Kerminen, K. Hameri, P. Vaattovaara, *Atmosph. Chem. Phys.* 5 (2005) 767.
- [11] H. Cruickshank, in: Proceedings of the Fifth International Conference on Satellite Systems Mobile Communication and Navigator, 1996, 187pp.
- [12] M. Hwang, C. Yang, C. Shiu, *ACM SIGOPS Oper. Syst. Rev.* 37 (2003) 42.
- [13] Y. Chang, C. Chang, *ACM SIGOPS Oper. Syst. Rev.* 39 (2003) 70.
- [14] V. Atluri, S. Chun, *IEEE Trans. Dependable Secure Comput.* 1 (2004) 238.
- [15] T. Peltier, *Information Security Risk Analysis*, second ed., Auerbach Publications, Boca Raton, FL, 2005.
- [16] M. Sahinoglu, *IEEE Secur. Privacy* 3 (2005) 18.
- [17] M. Berg, H.C. Tran, T.C. Nguyen, H. Pham, R. Schertenleib, W. Giger, *Environ. Sci. Technol.* 35 (2001) 2621.
- [18] M.F. Hossain, *Agric. Ecosyst. Environ.* 113 (2006) 1.
- [19] M.C. Shih, *Desalination* 172 (2005) 85.
- [20] US-EPA, EPA-542-S-02-002 (2002). US-EPA Office of Ground Water and Drinking Water, EPA Report-816-D-02-005, Cincinnati, OH, 2002.
- [21] WHO, *Guidelines for Drinking Water Quality. Recommendations*, third ed., WHO, Geneva, Switzerland, vol. 1, 2004.
- [22] I. Rau, A. Gonzalo, M. Valiente, *React. Funct. Polym.* 54 (2003) 85.
- [23] S. Shevade, R.G. Ford, *Water Res.* 38 (2004) 3197.
- [24] T.S. Singh, K.K. Pant, *Sep. Purif. Technol.* 36 (2004) 139.
- [25] B. Han, J. Zimbron, T.R. Runnells, Z. Shen, S.R. Wickramasinghe, *J. Am. Water Works Assoc.* 95 (2003) 109.
- [26] B. Han, T. Runnells, J. Zimbron, R. Wickamasinghe, *Desalination* 145 (2002) 293.
- [27] P.R. Kumar, S. Chaudhari, K.C. Khilar, S.P. Mahajan, *Chemosphere* 55 (2004) 1245.
- [28] S. Song, A. Lopez-Valdivieso, D.J. Hernandez-Campos, C. Peng, M.G. Monroy-Fernandez, I. Razo-Soto, *Water Res.* 40 (2006) 364.
- [29] R.Y. Ning, *Desalination* 143 (2002) 237.
- [30] D. Pokhrel, T. Viraraghavan, *Water Res.* 40 (2006) 549.
- [31] M. Kang, M. Kawasaki, S. Tamada, T. Kamei, Y. Magara, *Desalination* 131 (2000) 293.
- [32] Y. Sato, M. Kang, T. Kamei, Y. Magara, *Water Res.* 36 (2002) 3371.
- [33] S. Kundu, A.K. Gupta, *J. Colloid Interface Sci.* 290 (2005) 52.
- [34] I.A. Katsoyiannis, A.I. Zouboulis, *Water Res.* 38 (2004) 17.
- [35] A. Dutta, M. Chaudhuri, *J. Water SRT-Aqua* 40 (1991) 25.
- [36] L.A. Zeng, *Water Res.* 37 (2003) 4351.
- [37] J.A. Wilkie, J.G. Hering, *Colloids Surf. A* 107 (1996) 97.
- [38] K.P. Raven, A. Jain, R.H. Loeppert, *Environ. Sci. Technol.* 32 (1998) 344.
- [39] X. Sun, H.E. Doner, *Soil Sci.* 163 (1998) 278.
- [40] U. Schwertmann, *Cornell Rm. Iron Oxides in the Laboratory: Preparation and Characterization*, second completely revised and extended ed., Wiley, VCH, Weinheim, 2000.
- [41] S. Rutledge, M.M. Hohman, M.Y. Shin, M.P. Brenner, *Phys. Fluids* 13 (2001) 2201; S. Rutledge, M.M. Hohman, M.Y. Shin, M.P. Brenner, *Phys. Fluids* 13 (2001) 2221.